fermentation

Article

Electrode Material Optimization of Nitrous Oxide Recovery from Incineration Leachate in a Δ*nosZ Pseudomonas aeruginosa*/MEC System

Yong Liu [1], Bing Yan [1], Song Xia [1], Shuanglin Gui [1], Haiwei Jiang [1], Hanbing Nie [1,2,*] and Dezhi Sun [2]

[1] Institute of Energy, Jiangxi Academy of Science, Nanchang 330096, China; liuyong_aos@163.com (Y.L.); yanbing718@126.com (B.Y.); xiasongsummer212@163.com (S.X.); gsl503@163.com (S.G.); haiweij@126.com (H.J.)
[2] College of Environmental Science and Engineering, Beijing Forestry University, Beijing 100083, China; sdzlab@126.com
* Correspondence: niehanbing221@126.com

Abstract: Nitrous oxide (N_2O) is not only recognized as a potent greenhouse gas, but it is also used in industry as a clean energy source. In this study, different electrode materials of carbon felt and graphite were equipped in the Δ*nosZ P. aeruginosa*/microbial electrolysis cell (MEC) systems to explore the optimization mechanism for long-term N_2O recovery during incineration leachate treatment. The carbon felt group showed a better performance in N_2O recovery across 45 days of operation. The N_2O conversion efficiency was above 80% and the proportion of N_2O in biogas accounted for 80.6% in the carbon felt group. qRT-PCR analysis was conducted to evaluate the expression of genes involved in denitrification (*norB*) and electroactivity (*phzG*, *phzM*, and *phzH*) of Δ*nosZ P. aeruginosa*. The results showed a significant upregulation in the suspended biomass (day 21) and the electron-attached biomass (day 45) from the carbon felt-equipped reactor, which was highly related to the opportunity of biomass exposed to the phenazine derivatives. By the carbon felt optimization in the system, 82.6% of the *Pseudomonas* genus survived after 45 days of operation. These results indicate that the carbon felt electrode has a more sustainable performance for N_2O recovery in the Δ*nosZ P. aeruginosa*/MEC system.

Keywords: nitrous oxide; incineration leachate; *Pseudomonas aeruginosa*; denitrification; electroactivity

Citation: Liu, Y.; Yan, B.; Xia, S.; Gui, S.; Jiang, H.; Nie, H.; Sun, D. Electrode Material Optimization of Nitrous Oxide Recovery from Incineration Leachate in a Δ*nosZ Pseudomonas aeruginosa*/MEC System. *Fermentation* **2023**, *9*, 607. https://doi.org/10.3390/fermentation9070607

Academic Editor: Lijuan Zhang

Received: 19 May 2023
Revised: 11 June 2023
Accepted: 25 June 2023
Published: 28 June 2023

1. Introduction

Incineration leachate is a type of wastewater that contains high concentrations of organic matter (COD, 30,000~70,000 mg/L) and nitrogen (mainly NH_4^+-N, 1000~2000 mg/L), with a complex composition [1]. Typically, it is treated using a composite process of "pretreatment-biological treatment-advanced treatment" [2]. Organic matter and ammonia in the incineration leachate are primarily removed through the "anaerobic digestion-aerobic nitrification-anoxic denitrification" process in the biochemical treatment section. With the continuous advancement of wastewater resource research, most organic matter in incineration leachate can be converted into energy through optimized anaerobic digestion to produce methane [3,4]. However, research on the recovery of nitrogen resources is relatively scarce.

In the commonly used nitrification–denitrification process for nitrogen removal, a portion of the ammonia is converted into a controversial intermediate product known as nitrous oxide (N_2O). N_2O is a recognized potent greenhouse gas, but it has a higher calorific value when burned with CH_4 than O_2 and is also a clean energy source [5]. In unregulated wastewater treatment, the conversion efficiency of N_2O is only 0.11~1.90% [6–10], which cannot be recovered as energy and also causes the greenhouse effect. Therefore, by regulating the microbial metabolism involved in the nitrification–denitrification process, ammonia, nitrate, and nitrite in wastewater can be efficiently converted into N_2O and then collected. This not only achieves energy recovery of N_2O during wastewater denitrification treatment but also reduces greenhouse gas emissions from wastewater treatment plants.

Currently, some research is attempting to recover N_2O from wastewater. Coupled aerobic–anoxic nitrous decomposition operation (CANDO) induces heterotrophic denitrifying bacteria to store carbon sources in the form of polyhydroxyalkanoates (PHAs) in cells by alternately providing carbon and nitrogen sources in pulses. PHA does not easily provide electrons, resulting in the accumulation of N_2O, with a conversion rate of up to 87% [11]. A photocatalytic autotrophic denitrification system based on the combination of semiconductor CdS and *Thiobacillus* denitrificans can also achieve efficient conversion of N_2O. By utilizing the characteristic that sulfides can react with metal active centers, the activity of nitrous oxide reductase (Nos) was inhibited, resulting in a high N_2O conversion efficiency of 71% to 73.2% [12]. In a sulfur autotrophic denitrifying bacteria-dominated reactor, the NO, which was fixed by Fe(II)EDTA as the electron acceptor for denitrification, can inhibit the activity of Nos within an appropriate threshold, and achieved a 41% conversion of N_2O [13]. However, the above processes will also inhibit the activity of other enzymes while regulating the nitrogen converted to N_2O and limiting the efficiency of nitrogen removal. This defect will be further magnified when dealing with complex wastewater in practice. In a previous study, a denitrifying strain with high N_2O conversion performance, *Pseudomonas aeurginosa* PAO1, was constructed by knocking out *nosZ* (gene coding for Nos) [14]. With the *nosZ*-deficient strain of *P. aeurginosa* (Δ*nosZ P. aeurginosa*) supplied into the incineration leachate nitrogen removal process for microflora optimization, denitrification efficiency of 99% was achieved, and the N_2O conversion efficiency was as high as 95% [15]. The above results demonstrate the ability of Δ*nosZ P. aeurginosa* to deal with complex wastewater.

However, in order to efficiently convert N_2O by supplying Δ*nosZ P. aeruginosa* in the denitrification process, it is necessary to strengthen the dominant position of this functional bacterium. During long-term operation in a moving bed biofilm reactor (MBBR), the abundance of Δ*nosZ P. aeruginosa* was observed to decrease to 38% [15]. Subsequent research has found that using an MEC to stimulate Δ*nosZ P. aeruginosa* to secrete more phenazine derivatives can greatly improve its denitrification ability, biofilm formation rate, and survival advantage through the electron transfer ability, signaling molecule function, and antibacterial ability of phenazine derivatives [16]. Its abundance can be maintained at 66% in the Δ*nosZ P. aeruginosa*/MEC system. The process of indirect electron transfer between phenazine derivatives and electrodes by Δ*nosZ P. aeruginosa* may be a key factor in affecting its dominant position in the Δ*nosZ P. aeruginosa*/MEC system. Recent studies showed that phenazine could enhance the electron transport between *P. aeruginosa* PAO1 and a poised-potential electrode under anaerobic conditions [17]. Different electrode surfaces also influence phenazine production when *P. aeruginosa* requires electrode respiration [18]. However, few studies focus on the relationship between electroactivity and denitrification of *P. aeruginosa*. In a previous study, the electroactivity of *P. aeruginosa* was enhanced by supplying a quorum-sensing signal molecule, which resulted in a higher nitrogen removal efficiency and more stable N_2O conversion efficiency [19]. This method allows *P. aeruginosa* to generate more phenazines to transfer electrons, but the role of the electrode as the electron receiver is ignored. Therefore, the next step to improve the sustainability of this system for recovering N_2O is reveal the effect of electrode materials on the denitrification of Δ*nosZ P. aeurginosa*.

In this study, a carbon felt electrode and graphite electrode were set up in two Δ*nosZ P. aeurginosa*/MEC systems to investigate the effect of electrode materials on nitrogen conversion performance, gene expression involved in related processes, and the bacterial community structure in the Δ*nosZ P. aeurginosa*/MEC system. The goal is to further strengthen the dominant position of Δ*nosZ P. aeurginosa* from the perspective of electrode material optimization and achieve more efficient conversion of N_2O from incineration leachate.

2. Materials and Methods

2.1. Configuration of the ΔnosZ P. Aeruginosa/MEC System

The bioreactors used in this study were based on a two-chamber MEC construction (Figure 1). Each chamber of the reactors contains a liquid volume of 250 mL and a headspace volume of 150 mL. The working electrodes equipped in the anode chamber and the counter electrodes equipped in the cathode chamber were adopted with the same size of 60 × 30 × 5 mm whether formed with graphite material or carbon felt material. The specific surface area of graphite material and carbon felt material was 1.82 m^2/g and 2.34 m^2/g, respectively. Both the electrode materials were connected with a nickel rod before being applied into the microbial electrochemical system. Additionally, Ag/AgCl electrodes (+199 mv vs. SHE) saturated with KCl were also supplied in the anode chamber and reserved as the reference electrode. The anode potential was controlled using a potentiostat (Chil1030C, Shanghai, China). The anode and cathode chambers were separated by a 9.6 cm^2 anion exchange membrane (AEM, ASTOM Co., Tokyo, Japan).

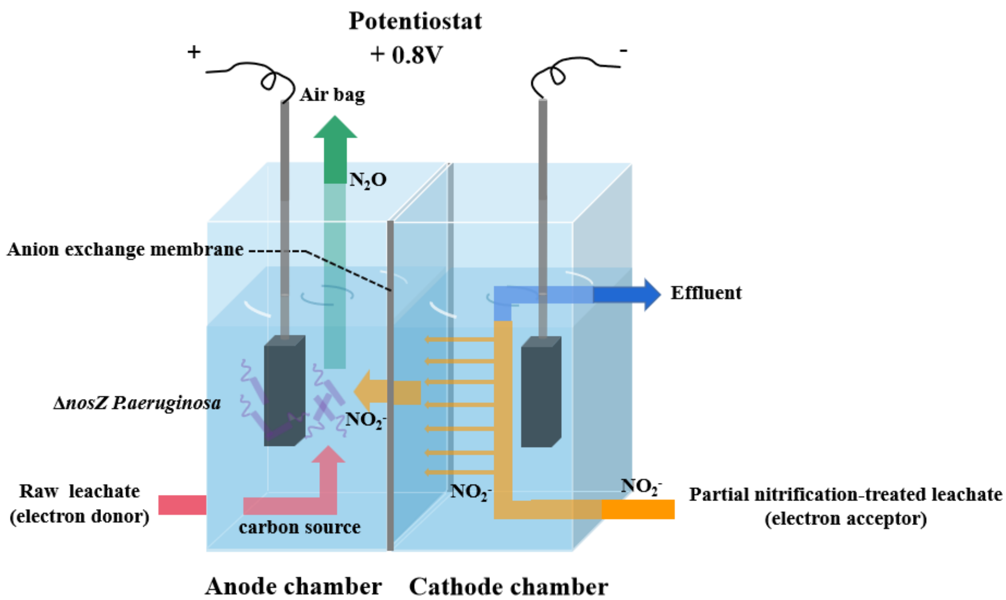

Figure 1. Schematic diagram of the Δ*nosZ P. aeruginosa*/MEC system.

The Δ*nosZ P. aeruginosa* strain was enriched in LB medium for 24 h at 37 °C and subsequently inoculated into a laboratory-scale MBBR for biofilm formation until the biomass attached to the polypropylene fillers (embedded with a cross-shaped carrier) reached 0.31 ± 0.02 mg per filler. Each anode chamber of the MEC reactors was supplied with 30 fillers immobilized with Δ*nosZ P. aeruginosa*. The raw incineration leachate was collected from an MSW energy incineration plant in Beijing and sterilized using a 0.22 µm filter to remove any microbes present in the leachate. The pre-treated incineration leachate was then supplied to the anode chamber as a carbon source for denitrification by Δ*nosZ P. aeruginosa*. The cathode chamber was continuously fed with partially nitrification-treated leachate, and nitrite that was able to pass through the AEM served as an electron acceptor for denitrification in the anode chamber. Characteristics of experimental wastewater used in this study are summarized in Table 1.

Table 1. Characteristics of experimental wastewater used in this study.

Item	COD (mg/L)	BOD5 (mg/L)	NH_4^+-N (mg/L)	NO_3^--N (mg/L)	NO_2^--N (mg/L)	pH
Raw leachate	57,686–75,480	23,858–33,710	968 ± 1368	N/A	N/A	6.01–6.37
Anaerobically treated leachate	1820–4625	879–3182	1029–1458	N/A	N/A	7.95–8.45
Partial nitrification-treated leachate	1524–2123	97–334	178–204	21.78–35.53	945–1125	7.27–7.93

2.2. Experimental Set-Up

Two Δ*nosZ P. aeruginosa*/MEC systems with carbon felt electrodes and graphite electrodes were used in this study. Both experimental groups were used under the same manner. The operation temperature was maintained in the range of 30 ± 1 °C. The anode potential applied in this study was +0.8 V. The concentration of NO_2^--N in partial nitrification-treated leachate was ~1000 mg/L when it served as the inflow of the cathode chamber.

In the process of the experiment, the hydraulic retention time (HRT) was gradually shortened, and it depended on the NO_2^--N removal efficiency of Δ*nosZ P. aeruginosa* of each group. The NO_2^--N concentrations of the anode chamber and cathode chamber in each group were monitored daily. The NO_2^--N removal efficiency, which reflected the overall nitrite removal performance of the Δ*nosZ P. aeruginosa*/MEC system, and the N_2O conversion efficiency, which reflected the N_2O conversion capabilities of the Δ*nosZ P. aeruginosa*, were calculated with the equation described in a previous study [16].

2.3. RNA Extraction and Quantitative Reverse Transcription PCR (qRT-PCR)

Microbial cells in a suspended state and the anode electrode were harvested on day 21 and day 45, respectively. A centrifuge operating at 8000 rpm for 10 min was used to concentrate the cells, which were then used for RNA extraction using the RNAprep Bacteria Kit (Aidlab Biotechnologies, China). To ensure RNA purity, an additional step was taken to remove residual DNA using DNA-free DNase (New England Biolabs, Beijing, China) following the manufacturer's instructions.

Purified RNA (1 µg) was used to synthesize cDNA through reverse transcription using the THERMOscript 1st Strand cDNA Synthesis Kit (Aidlab Biotechnologies, Beijing, China) according to the manufacturer's instructions. The resulting cDNA products were used as templates for quantitative polymerase chain reaction (qPCR) with primers targeting genes involved in denitrification and phenazine biosynthesis, as well as the constitutively expressed housekeeping gene *proC*. qPCR detection was performed using a real-time PCR system (7500 FAST, USA), as previously described [15,16,19].

2.4. DNA Extraction and Sequence Analysis

On days 21 and 45, microbial cells growing in the anode chamber of the Δ*nosZ P. aeruginosa*/MEC system were harvested for DNA extraction using the RNeasy PowerSoil DNA elution kit (QIAGEN), following the manufacturer's instructions. The concentration and purity of the extracted DNA samples were determined using the Nanodrop UV spectrophotometer (Thermo Fisher Scientific, Delaware).

Bacterial 16S rRNA gene fragments were amplified via PCR using the 338F/806R primer set. The resulting amplicons were sequenced on an Illumina Hiseq 2000 platform (Illumina, San Diego, CA, USA) by Majorbio Bio-Pharm Technology Co., Ltd. (Shanghai, China). The sequences were then sorted into various operational taxonomic units using Pyrosequencing Pipeline software (https://pyro.cme.msu.edu) accessed on 3 July 2021. The raw sequence files have been deposited in the NCBI Sequence Read Archive database under accession NO. PRJNA974214.

2.5. Analytical Methods

In this study, the water quality index, including NO_2^--N and COD concentrations, was determined using standard methods (APHA, 2005). The measurement of N_2O followed a previous study [16]. To measure the biomass in the middle of a continuous experiment, two parallel reactors of carbon felt and graphite were used. When measuring the biomass, the biomass of all states was collected from the parallel reactors. The immobilized biomass and the biomass on the electrode were measured for dry weight after scraping or squeezing until cells were no longer obtained from the carriers. The biomass in suspended state was measured through the linear relation between OD600 and biomass [19]. Phenazine derivatives in the anode chamber were extracted using chloroform and then re-extracted using deionized water with different pH levels. The concentration of phenazine-1-carboxylic acid (PCA), 1-hydrophenazine(1-OH-PHZ), and pyocyanin (PYO) were determined using the linear relation between the standard substance and absorbency under 252 nm (neutral), 520 nm (alkaline), and 520 nm (acidic), respectively [20,21].

3. Results

3.1. Performance of ΔnosZ P. aeruginosa/MEC Reactors with Carbon Felt Electrodes and Graphite Electrodes

The Δ*nosZ P. aeruginosa*/MEC systems with carbon felt electrodes and graphite electrodes were operated for 45 days, and the influent NO_2^--N concentration of partial nitrification-treated incineration leachate was about 1000 mg/L (Figure 2). From day 1 to day 9, the NO_2^--N removal efficiency of two groups of reactors gradually increased to 83.3% and 78.1%, respectively, through the enrichment of Δ*nosZ P. aeruginosa* in the anode chamber. In the subsequent stage (from day 9 to day 33), the HRT was reduced to 6 days, and the average cathode NO_2^--N effluent concentrations of the carbon felt group and graphite group reactors were 183.3 mg/L and 234.9 mg/L, respectively. The carbon felt group exhibited an average TN removal rate of 81.92%, which was 6.63% higher than that of the graphite group (Figure 2). On day 33, the HRT was further shortened to 3 days. At this point, the cathode NO_2^--N effluent concentration of the two groups of MEC reactors increased due to the mass transfer capacity of the anion exchange membrane reaching its upper limit, with average values of 239.3 mg/L and 294.4 mg/L, respectively. The average NO_2^--N removal rate decreased to 76.22% and 69.66%, but the carbon felt group still exhibited a 6.56% higher NO_2^--N removal rate than the graphite group (Figure 2).

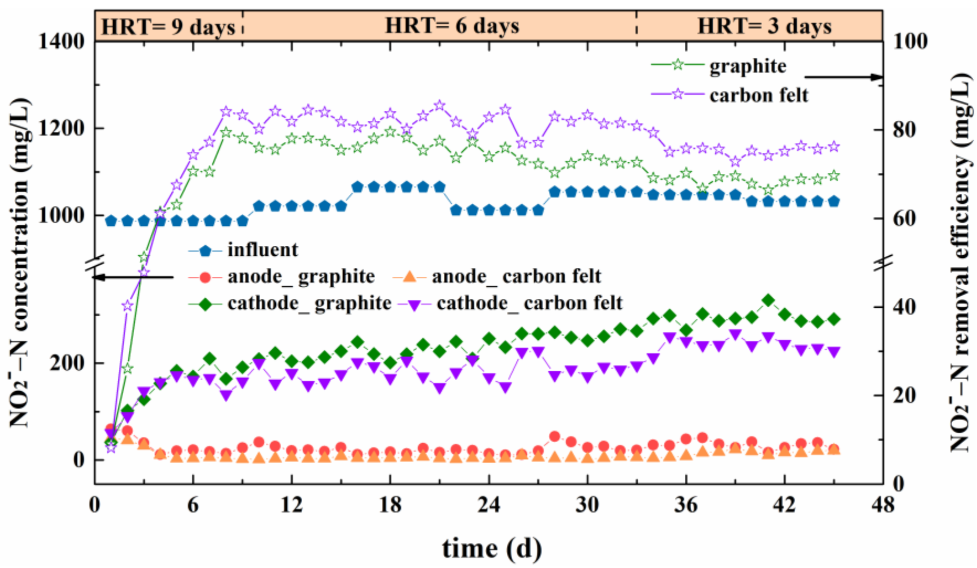

Figure 2. Nitrite removal of Δ*nosZ P. aeruginosa*/MEC systems with carbon felt electrodes and graphite electrodes.

Based on the N_2O conversion performance of the Δ*nosZ P. aeruginosa*/MEC system with two different electrode materials (Figure 3), there was no significant difference in gaseous N_2O production (4.05 ± 0.04 mmol) between the carbon felt and graphite groups from day 1 to day 21. However, the N_2O conversion efficiency of the carbon felt group was 5.18% lower than that of the graphite group, indicating that the N_2O conversion process by Δ*nosZ P. aeruginosa* in the carbon felt group reactor was interfered with during this stage. Subsequently, after day 21, the N_2O conversion performance of the carbon felt group reactor gradually surpassed that of the graphite group. The average gaseous N_2O production was higher in the carbon felt group than in the graphite group by 0.51 ± 0.02 mmol, with the highest difference observed on day 45 (0.83 ± 0.03 mmol). Additionally, the N_2O in the carbon felt group remained above 80%, while there was a downward trend in the graphite plate group after day 39 of operation (Figure 3). The proportion of N_2O in biogas production represents its recovery potential, and on day 45, N_2O accounted for 80.6% of biogas production in the carbon felt group, which was 16.8% higher than that in the graphite group (Figure 3).

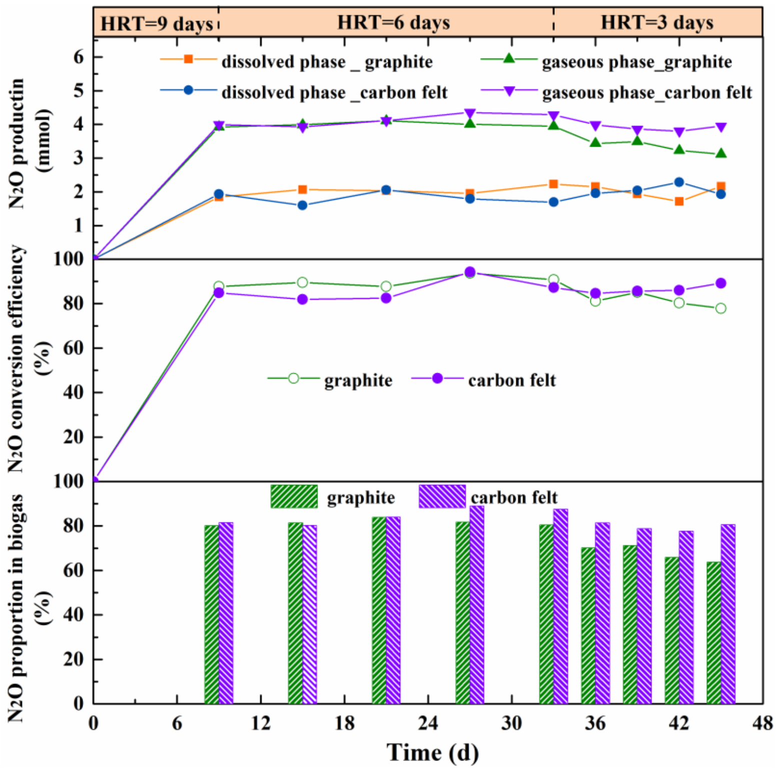

Figure 3. Nitrous oxide conversion of Δ*nosZ P. aeruginosa*/MEC systems with carbon felt electrodes and graphite electrodes. (**a**) N_2O production; (**b**) N_2O conversion efficiency; (**c**) N_2O proportion in biogas. Error bars represent standard deviations of triplicate measurements.

The above findings suggest that the carbon felt may be a more effective anode electrode material for the Δ*nosZ P. aeruginosa*/MEC system in terms of N_2O conversion performance and recovery potential. Further research is needed to investigate the underlying mechanisms behind these observations.

3.2. Effect of Electrode Materials on Denitrification, Electroactivity, and Biomass of ΔnosZ P. aeruginosa

qRT-PCR analysis was performed for expression of denitrification and electroactivity genes in Δ*nosZ P. aeruginosa*/MEC systems with carbon felt electrodes and graphite electrodes (Figure 4). The transcription of the *norB* gene of the terminal nitric oxide reductase of Δ*nosZ P. aeruginosa* is shown in Figure 4a. Gene expression of *norB* in both groups of reactors increased on day 45 compared to day 21, indicating that electric stimulation gradually enhanced the effect on Δ*nosZ P. aeruginosa*. By comparing the gene expression of suspended bacteria, it can be observed that the difference multiple of norB expression between the carbon felt group and the graphite group gradually decreased from 3.08 times on day 21 to 1.11 times on day 45 (Figure 4a). The expression levels of *phzG*, *phzM*, and *phzH* involved in regulating phenazine derivative synthesis in suspended bacteria in the carbon felt group decreased on day 45 compared to day 21, but the opposite was true for the graphite group. The biomass results indicate that the gap between the biomass of suspended bacteria in both groups increased on day 45, with 74.83 ± 2.21 mg and 56.28 ± 2.54 mg for the carbon felt group and graphite group, respectively (Figure 5a). On day 45, the value of total phenazine derivative per unit biomass accessible by the carbon felt group (0.096 ± 0.002) was not significantly different from that of the graphite group (0.085 ± 0.006) (Figure 5b). The reason for this result may be that the biomass attached to the surface of the carbon felt electrode is higher (2.42 times that of the graphite group), which excessively occupies the opportunity for suspended bacteria to use phenazine derivatives for electron transfer with electrodes. The advantage of the carbon felt group over the graphite group for suspended bacteria lies mainly in higher synthesis of phenazine in early operation, which promotes biomass increase.

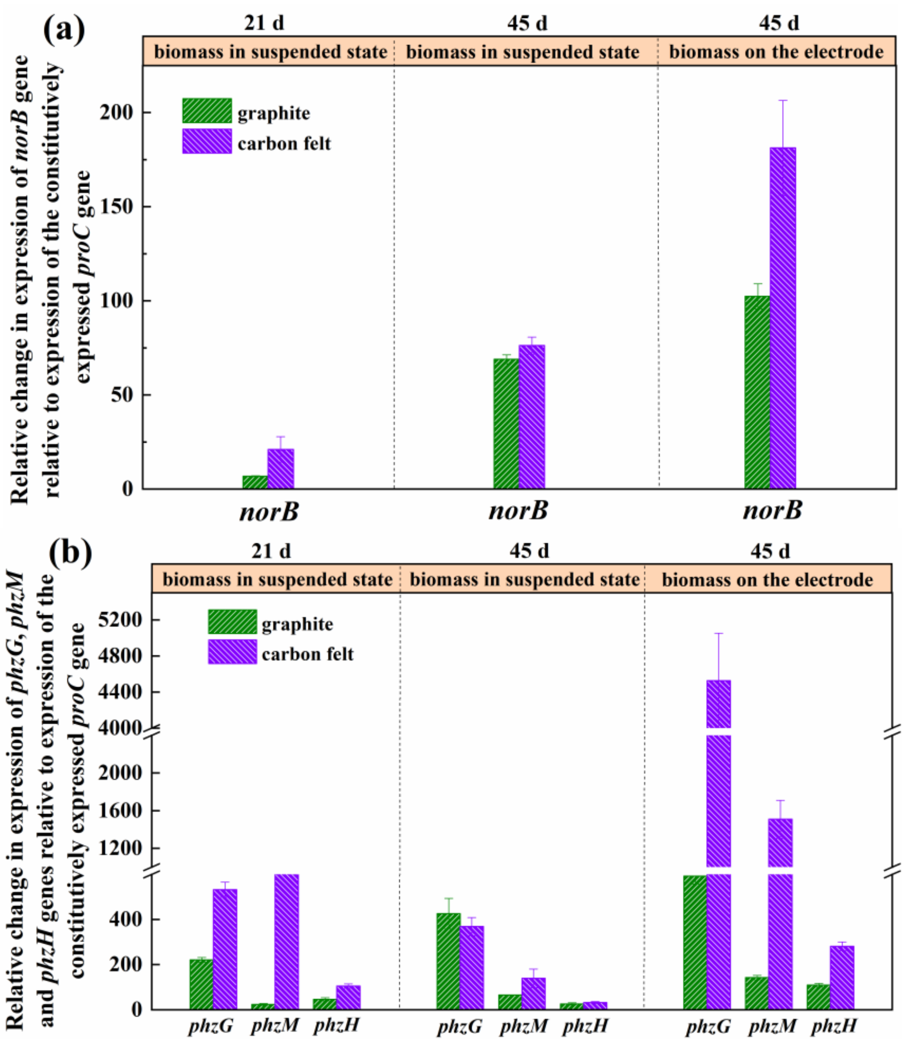

Figure 4. Denitrification- and electroactivity-related gene expression in the Δ*nosZ P. aeruginosa*/MEC systems with carbon felt electrodes and graphite electrodes on day 21 and 45. (**a**) *norB*; (**b**) *phzG*, *phzM*, and *phzH*. Error bars represent standard deviations of triplicate measurements.

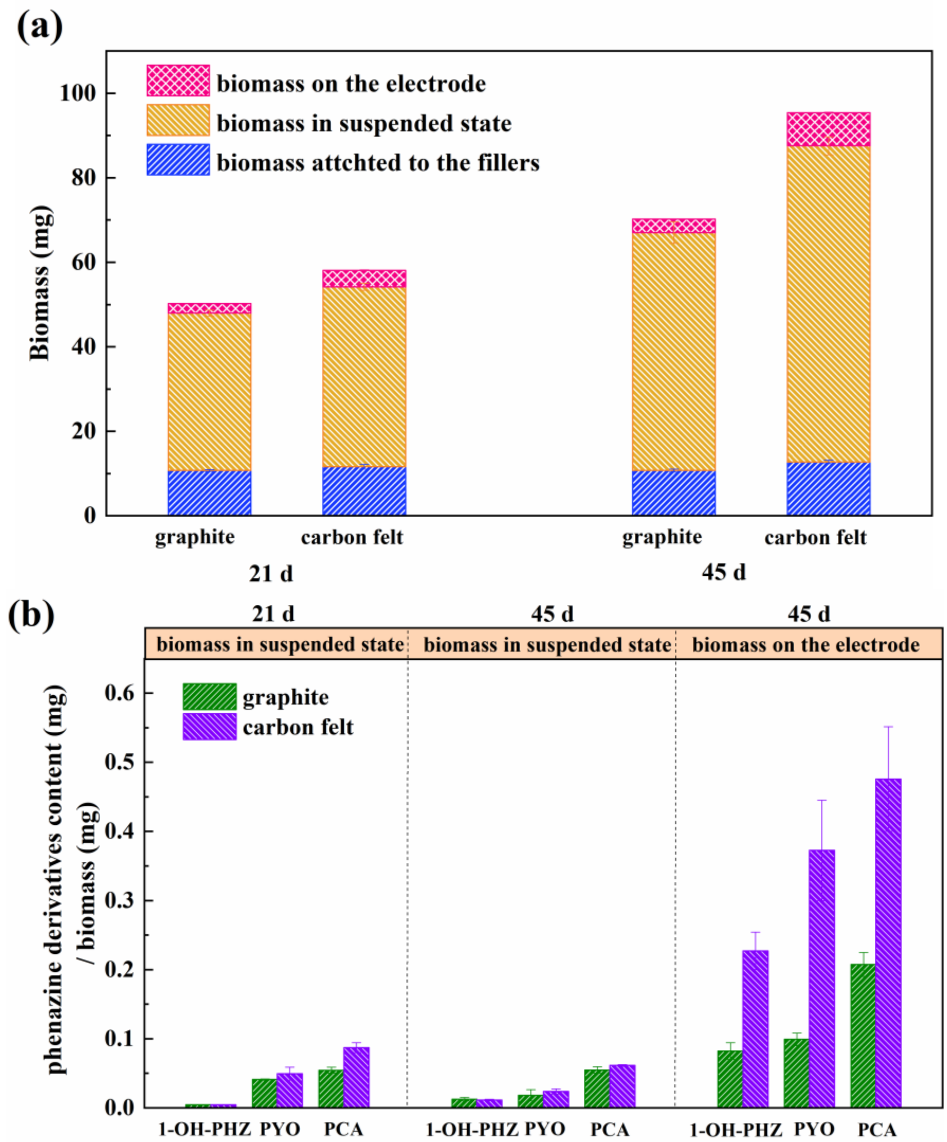

Figure 5. Biomass and the opportunity of touching phenazine derivatives per unit of biomass in the Δ*nosZ P. aeruginosa*/MEC systems with carbon felt electrodes and graphite electrodes on day 21 and 45. (**a**) Biomass; (**b**) phenazine derivative content/biomass. Error bars represent standard deviations of triplicate measurements.

On day 45 of operation, the *norB* gene expression of electrode-attached and suspended Δ*nosZ P. aeruginosa* was compared. The *norB* gene expression of Δ*nosZ P. aeruginosa* on the carbon felt electrode was found to be much higher than that of the suspended state (2.73 times), as shown in Figure 4a. Additionally, the gene expression levels of *phzG*, *phzM*, and *phzH* of Δ*nosZ P. aeruginosa* attached to the carbon felt electrode were 7.64 times, 10.61 times, and 2.59 times that of the graphite plate group, respectively (Figure 4b). The total phenazine derivative per unit biomass accessible by the carbon felt group was more than twice that of the graphite plate group. These results suggest that the carbon felt electrode is more effective than the graphite electrode in promoting the denitrification process and electrode respiration of Δ*nosZ P. aeruginosa*.

3.3. Bacterial Community Analysis

The bacterial community structure enriched under the influence of two different electrode materials is analyzed in Figure 6. On day 21 of operation, the abundance of the *Pseudomonas* genus in the carbon felt group was high, at 91.7%, while that in the graphite group was 82.9%. Furthermore, it was observed that more genera appeared in the carbon felt group, such as *Alkaliphilus* (4.57%), *Eubacterium* (2.94%), and *Citrobacter* (0.76%). *Alkaliphilus* can convert nitrite nitrogen in the system into ammonia nitrogen through dissimilatory nitrate reduction [22] and has been found to be enriched in heterotrophic denitrifying microbial fuel cells [23], but it does not have denitrifying function. Therefore, the decrease in N_2O conversion rate in the carbon felt group in Figure 3 is due to *Alkaliphilus* in the community converting part of the nitrite into ammonia nitrogen. *Eubacterium* does not have any genes related to denitrification, but it is related to AI-2 type signal molecule-induced quorum sensing [24,25], which may be related to the *lux* quorum-sensing system regulated by the *luxS* gene carried by *Eubacterium* [26]. This has a synergistic effect on quorum sensing with the *Pseudomonas* genus.

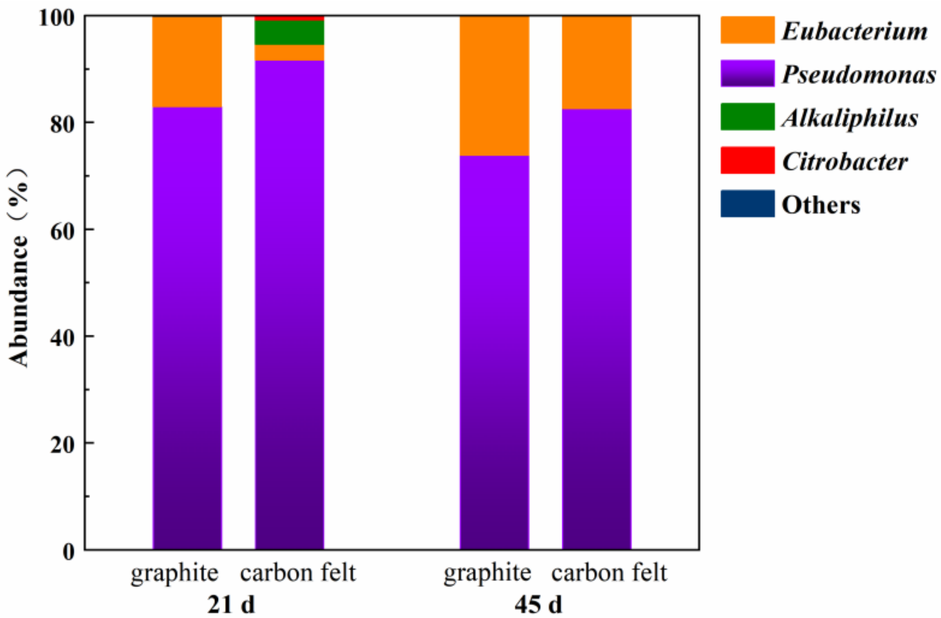

Figure 6. Bacterial community analysis on anode of the Δ*nosZ P. aeruginosa*/MEC systems on day 21 and 45.

On day 45 of operation, the abundance of *Pseudomonas* genus in the carbon felt group and graphite group was 82.6% and 73.8%, respectively, both decreased compared to day 21. The abundance of *Pseudomonas* genus in the carbon felt group remained relatively high, and it was found that the *Alkaliphilus* and *Citrobacter* originally present in the community disappeared, indicating that these invading genera gradually became unsuitable for the environment within the MEC reactor with its operation, which may be related to the antibacterial effect of some secondary metabolites secreted by *Pseudomonas*. In addition, *Eubacterium* still exists as a heterotrophic bacterium producing N_2O from denitrification in both MEC reactors, indicating that there is indeed a synergistic symbiotic relationship between *Eubacterium* and *Pseudomonas* genus.

4. Discussion

The Δ*nosZ P. aeruginosa*/MEC system with carbon felt electrodes has shown 5~6% improvement of nitrite removal and N_2O conversion efficiencies compare to the one equipped with graphite electrodes. In this system, as described in Figure 1, nitrite in partial nitrification-treated leachate needs to pass through the AEM and then be utilized by the Δ*nosZ P. aeruginosa* as the electron acceptor for denitrification. There are two ways to impact the nitrite consumption, that is, the electrode attraction by the anode and the denitrification ability of Δ*nosZ P. aeruginosa.* However, a previous study confirmed that the electrode attraction showed little effect on nitrite transfer from the cathode chamber to the anode chamber. Therefore, the denitrification ability of Δ*nosZ P. aeruginosa* is the major approach to illustrate the improvement by carbon felt electrodes. In the denitrification pathway of Δ*nosZ P. aeruginosa*, *norB* is the terminal gene which regulates the NO converted to N_2O. qRT-PCR results of the *norB* can represent the denitrification ability of the individual Δ*nosZ P. aeruginosa* cell and showed a high expression in the carbon felt group at the early operation phase (day 21, biomass in suspended state) and the end of operation (day 45, biomass attached on electrode). It revealed that the carbon felt may better enhance the denitrification of the Δ*nosZ P. aeruginosa* cell by establishing a more efficient electron transfer chain. Otherwise, the cells with higher expression of *norB* will not be found in the conditions that possess the maximum chance of contact with the electrode. Meanwhile, this could easily imply that the nitrogen removal performance not only depends on the ability of individual cells but also relates to the biomass quantity of Δ*nosZ P. aeruginosa*. Fortunately, the biofilm formation of Δ*nosZ P. aeruginosa* has a deep connection with a type of signal molecule, called phenazine derivates [27,28]. Phenazine derivates also play an important part in the indirect electron transfer between the Δ*nosZ P. aeruginosa* cells and electrode [16,17,29,30]. The higher concentrations of phenazine derivates and much more expressed genes of phenazine derivates synthesis were also found in the same conditions (day 21, biomass in suspended state and day 45, biomass attached on electrode), in accordance with *norB* expression and the biomass in the carbon felt group. The results showed a strong correlation among the denitrification, electroactivity, and biomass in Δ*nosZ P. aeruginosa*. Phenazine derivates are key compounds of the two electrode materials and showed differences in the coupled systems.

The improvement of N_2O conversion by using carbon felt electrodes in the Δ*nosZ P. aeruginosa*/MEC system is the major finding for achieving the long-term recovery of N_2O from incineration leachate. A total of 82.6% of the *Pseudomonas* genus survived, with the other genus eliminated in the carbon felt group. It may relate to the antibiotic characteristics of phenazine derivates or the gradually enhanced advantages during the operation process [31–34]. In conclusion, multiple results support the fact that carbon felt can optimize the Δ*nosZ P. aeruginosa*/MEC system predictably. Further study needs to explore the microbial electrochemical characteristics when operating the Δ*nosZ P. aeruginosa*/MEC system with the carbon felt electrode.

5. Conclusions

In this study, two Δ*nosZ P. aeruginosa* /MEC systems equipped with carbon felt electrodes and graphite electrodes were operated to analyze the optimization mechanism of electrode materials for N_2O recovery during incineration leachate treatment. The carbon felt group showed better performance in N_2O recovery during the 45-day operation, with N_2O conversion efficiency above 80% and the proportion of N_2O in biogas accounting for 80.6%. qRT-PCR analysis was conducted to evaluate the expression of genes involved in denitrification (*norB*) and electroactivity (*phzG*, *phzM*, and *phzH*) of Δ*nosZ P. aeruginosa*. The results showed significant upregulation in the suspended biomass (day 21) and the electron-attached biomass (day 45) from the carbon felt-equipped reactor, which was highly related to the opportunity of biomass exposed to the phenazine derivatives. The carbon felt group also had a higher survival rate of 82.6% of the *Pseudomonas* genus after 45 days of operation (8.8% higher than the graphite group). These results indicate that the carbon felt electrode has a more sustainable performance for N_2O recovery in the Δ*nosZ P. aeruginosa*/MEC system.

Author Contributions: Conceptualization, D.S. and H.N.; methodology, H.N.; software, S.G.; validation, H.J.; formal analysis, H.J.; investigation, Y.L.; resources, H.N. and D.S.; data curation, Y.L.; writing—original draft preparation, Y.L. and H.N.; writing—review and editing, B.Y. and S.X.; visualization, Y.L.; supervision, D.S. and H.N.; project administration, D.S. and H.N.; funding acquisition, D.S., B.Y. and S.X. All authors have read and agreed to the published version of the manuscript.

Funding: This research was funded by the National Natural Science Foundation of China, grant number 51678051; the Jiangxi Provincial Natural Science Foundation, grant number 20212BAB213042; Excellent Youth Training Program of Jiangxi Academy of Sciences, grant number 2022YSBG50006 and Introduction of Doctor Program of Jiangxi Academy of Sciences, grant number 2023YYB02.

Institutional Review Board Statement: Not applicable.

Informed Consent Statement: Not applicable.

Data Availability Statement: Not applicable.

Conflicts of Interest: The authors declare no conflict of interest.

References

1. Liu, X.Y.; Shu, Z.F.; Sun, D.Z.; Dang, Y.; Holmes, D.E. Heterotrophic Nitrifiers Dominate Reactors Treating Incineration Leachate with High Free Ammonia Concentrations. *ACS Sustain. Chem. Eng.* **2018**, *6*, 15040–15049. [CrossRef]
2. Chen, W.M.; He, C.; Zhuo, X.C.; Wang, F.; Li, Q.B. Comprehensive evaluation of dissolved organic matter molecular transformation in municipal solid waste incineration leachate. *Chem. Eng. J.* **2020**, *400*, 126003. [CrossRef]
3. Liu, C.Q.; Sun, D.Z.; Zhao, Z.Q.; Dang, Y.; Holmes, D.E. Methanothrix enhances biogas upgrading in microbial electrolysis cell via direct electron transfer. *Bioresour. Technol.* **2019**, *291*, 121877. [CrossRef] [PubMed]
4. Liu, C.A.Q.; Xiao, J.W.; Li, H.Y.; Chen, Q.; Sun, D.Z.; Cheng, X.; Li, P.S.; Dang, Y.; Smith, J.A.; Holmes, D.E. High efficiency in-situ biogas upgrading in a bioelectrochemical system with low energy input. *Water Res.* **2021**, *197*, 117055. [CrossRef] [PubMed]
5. Scherson, Y.D.; Wells, G.F.; Woo, S.G.; Lee, J.; Park, J.; Cantwell, B.J.; Criddle, C.S. Nitrogen removal with energy recovery through N2O decomposition. *Energy Environ. Sci.* **2013**, *6*, 241–248. [CrossRef]
6. Castellano-Hinojosa, A.; Maza-Marquez, P.; Melero-Rubio, Y.; Gonzalez-Lopez, J.; Rodelas, B. Linking nitrous oxide emissions to population dynamics of nitrifying and denitrifying prokaryotes in four full-scale wastewater treatment plants. *Chemosphere* **2018**, *200*, 57–66. [CrossRef]
7. Daelman, M.R.J.; De Baets, B.; van Loosdrecht, M.C.M.; Volcke, E.I.P. Influence of sampling strategies on the estimated nitrous oxide emission from wastewater treatment plants. *Water Res.* **2013**, *47*, 3120–3130. [CrossRef]
8. Duan, H.R.; van den Akker, B.; Thwaites, B.J.; Peng, L.; Herman, C.; Pan, Y.T.; Ni, B.J.; Watt, S.; Yuan, Z.G.; Ye, L. Mitigating nitrous oxide emissions at a full-scale wastewater treatment plant. *Water Res.* **2020**, *185*, 116196. [CrossRef]
9. Hwang, K.L.; Bang, C.H.; Zoh, K.D. Characteristics of methane and nitrous oxide emissions from the wastewater treatment plant. *Bioresour. Technol.* **2016**, *214*, 881–884. [CrossRef]
10. Kosonen, H.; Heinonen, M.; Mikola, A.; Haimi, H.; Mulas, M.; Corona, F.; Vahala, R. Nitrous Oxide Production at a Fully Covered Wastewater Treatment Plant: Results of a Long-Term Online Monitoring Campaign. *Environ. Sci. Technol.* **2016**, *50*, 5547–5554. [CrossRef]
11. Wang, Z.Y.; Woo, S.G.; Yao, Y.; Cheng, H.H.; Wu, Y.J.; Criddle, C.S. Nitrogen removal as nitrous oxide for energy recovery: Increased process stability and high nitrous yields at short hydraulic residence times. *Water Res.* **2020**, *173*, 115575. [CrossRef]
12. Chen, M.; Zhou, X.F.; Yu, Y.Q.; Liu, X.; Zeng, R.J.X.; Zhou, S.G.; He, Z. Light-driven nitrous oxide production via autotrophic denitrification by self-photosensitized Thiobacillus denitrificans. *Environ. Int.* **2019**, *127*, 353–360. [CrossRef] [PubMed]
13. Wu, L.; Wang, L.K.; Wei, W.; Song, L.; Ni, B.J. Sulfur-driven autotrophic denitrification of nitric oxide for efficient nitrous oxide recovery. *Biotechnol. Bioeng.* **2022**, *119*, 257–267. [CrossRef]
14. Lin, Z.Y.; Sun, D.Z.; Dang, Y.; Holmes, D.E. Significant enhancement of nitrous oxide energy yields from wastewater achieved by bioaugmentation with a recombinant strain of Pseudomonas aeruginosa. *Sci. Rep.* **2018**, *8*, 1–9. [CrossRef] [PubMed]
15. Nie, H.B.; Liu, X.Y.; Dang, Y.; Ji, Y.N.; Sun, D.Z.; Smith, J.A.; Holmes, D.E. Efficient nitrous oxide recovery from incineration leachate by a nosZ-deficient strain of Pseudomonas aeruginosa. *Bioresour. Technol.* **2020**, *297*, 122371. [CrossRef] [PubMed]
16. Nie, H.B.; Dang, Y.; Yan, H.K.; Sun, D.Z.; Holmes, D.E. Enhanced recovery of nitrous oxide from incineration leachate in a microbial electrolysis cell inoculated with a nosZ-deficient strain of Pseudomonas aeruginosa. *Bioresour. Technol.* **2021**, *333*, 125082. [CrossRef]
17. Guan, F.; Yuan, X.C.; Duan, J.Z.; Zhai, X.F.; Hou, B.R. Phenazine enables the anaerobic respiration of Pseudomonas aeruginosa via electron transfer with a polarised graphite electrode. *Int. Biodeterior. Biodegrad.* **2019**, *137*, 8–13. [CrossRef]
18. Slate, A.J.; Hickey, N.A.; Butler, J.A.; Wilson, D.; Liauw, C.M.; Banks, C.E.; Whitehead, K.A. Additive manufactured graphene-based electrodes exhibit beneficial performances in Pseudomonas aeruginosa microbial fuel cells. *J. Power Sources* **2021**, *499*, 229938. [CrossRef]
19. Nie, H.B.; Liu, X.Y.; Dang, Y.; Sun, D.Z. Early activated quorum sensing enhanced a nosZ-deficient strain of Pseudomonas aeruginosa for stably recovering nitrous oxide from incineration leachate in microbial electrolysis cell. *Bioresour. Technol.* **2022**, *360*, 127394. [CrossRef]
20. Cui, Q.N.; Lv, H.N.; Qi, Z.Z.; Jiang, B.; Xiao, B.; Liu, L.D.; Ge, Y.H.; Hu, X.M. Cross-Regulation between the phz1 and phz2 Operons Maintain a Balanced Level of Phenazine Biosynthesis in Pseudomonas aeruginosa PAO1. *PLoS ONE* **2016**, *11*, e0144447. [CrossRef]

21. Liang, H.H.; Li, L.L.; Dong, Z.L.; Surette, M.G.; Duan, K.M. The YebC family protein PA0964 negatively regulates the Pseudomonas aeruginosa quinolone signal system and pyocyanin production. *J. Bacteriol.* **2008**, *190*, 6217–6227. [CrossRef] [PubMed]
22. Thorup, C.; Schramm, A.; Findlay, A.J.; Finster, K.W.; Schreiber, L. Disguised as a Sulfate Reducer: Growth of the Deltaproteobacterium Desulfurivibrio alkaliphilus by Sulfide Oxidation with Nitrate. *Mbio* **2017**, *8*, e00671-17. [CrossRef] [PubMed]
23. Vijay, A.; Chhabra, M.; Vincent, T. Microbial community modulates electrochemical performance and denitrification rate in a biocathodic autotrophic and heterotrophic denitrifying microbial fuel cell. *Bioresour. Technol.* **2019**, *272*, 217–225. [CrossRef] [PubMed]
24. Lukas, F.; Gorenc, G.; Kopecny, J. Detection of possible AI-2-mediated quorum sensing system in commensal intestinal bacteria. *Folia Microbiol.* **2008**, *53*, 221–224. [CrossRef]
25. Mitsumori, M.; Xu, L.M.; Kajikawa, H.; Kurihara, M.; Tajima, K.; Hai, J.; Takenaka, A. Possible quorum sensing in the rumen microbial community: Detection of quorum-sensing signal molecules from rumen bacteria. *Fems Microbiol. Lett.* **2003**, *219*, 47–52. [CrossRef]
26. Ghali, I.; Shinkai, T.; Mitsumori, M. Mining of luxS genes from rumen microbial consortia by metagenomic and metatranscriptomic approaches. *Anim. Sci. J.* **2016**, *87*, 666–673. [CrossRef]
27. Price-Whelan, A.; Dietrich, L.E.P.; Newman, D.K. Rethinking 'secondary' metabolism: Physiological roles for phenazine antibiotics. *Nat. Chem. Biol.* **2006**, *2*, 221. [CrossRef]
28. Ramos, I.; Dietrich, L.E.P.; Price-Whelan, A.; Newman, D.K. Phenazines affect biofilm formation by Pseudomonas aeruginosa in similar ways at various scales. *Res. Microbiol.* **2010**, *161*, 187–191. [CrossRef]
29. Bosire, E.M.; Rosenbaum, M.A. Electrochemical Potential Influences Phenazine Production, Electron Transfer and Consequently Electric Current Generation by Pseudomonas aeruginosa. *Front. Microbiol.* **2017**, *8*, 892. [CrossRef]
30. Rabaey, K.; Boon, N.; Hofte, M.; Verstraete, W. Microbial phenazine production enhances electron transfer in biofuel cells. *Environ. Sci. Technol.* **2005**, *39*, 3401–3408. [CrossRef]
31. Firn, R.D.; Jones, C.G. Natural products—A simple model to explain chemical diversity. *Nat. Prod. Rep.* **2003**, *20*, 382–391. [CrossRef] [PubMed]
32. Jin, Z.J.; Zhou, L.; Sun, S.; Cui, Y.; Song, K.; Zhang, X.H.; He, Y.W. Identification of a Strong Quorum Sensing- and Thermo-Regulated Promoter for the Biosynthesis of a New Metabolite Pesticide Phenazine-1-carboxamide in Pseudomonas strain PA1201. *ACS Synth. Biol.* **2020**, *9*, 1802–1812. [CrossRef] [PubMed]
33. Sun, X.W.; Xu, Y.; Chen, L.; Jin, X.M.; Ni, H. The salt-tolerant phenazine-1-carboxamide-producing bacterium Pseudomonas aeruginosa NF011 isolated from wheat rhizosphere soil in dry farmland with antagonism against Fusarium graminearum. *Microbiol. Res.* **2021**, *245*, 126673. [CrossRef] [PubMed]
34. Wang, Y.; Kern, S.E.; Newman, D.K. Endogenous Phenazine Antibiotics Promote Anaerobic Survival of Pseudomonas aeruginosa via Extracellular Electron Transfer. *J. Bacteriol.* **2010**, *192*, 365–369. [CrossRef] [PubMed]